

Clustering of Meter-wave Luminous Objects toward Monoceros

Shuji DEGUCHI, and Kazutaka KOIKE

*Nobeyama Radio Observatory, National Astronomical Observatory,
and Department of Astronomical Science, The Graduate University for Advanced Studies,
Minamimaki, Minamisaku, Nagano 384-1305*

[PASJ (Letter) 60 No. 6 (Dec. 25, 2008 issue) in press]

(Received 2008 March 28; accepted 2008 September 11)

Abstract

A distribution of the meter-wave luminous objects, which are bright at frequency 74 MHz (a wavelength of 4 m) but not detectable at 1.4 GHz (21 cm) in the VLA surveys, shows a notable concentration in a scale of a few degrees toward Monoceros [(l, b)=(225°, 4°)]. We argue that it is a part of giant radio relics associated with a nearby cluster of galaxies with $cz \sim 2400$ km s⁻¹ centered on the spiral galaxy NGC 2377. The angular separation of these objects from the clustering center is consistent with the separation of distant relics to the cluster center if scaled by distance. This fact implies that the concentrations of meter-wave luminous objects can be used as a tracer of the structure of the Local Supercluster and its vicinity.

Key words: galaxies: clusters: general — radio continuum: galaxies— X-rays: galaxies: clusters

1. Introduction

The nature of very low frequency radio sources are not well investigated. Especially, objects detected by the VLA Low-frequency Sky Survey (VLSS; Cohen et al. 2007) at 74 MHz, but without the 1.4 GHz NRAO VLA Sky Survey (NVSS; Condon et al. 1998) association, are quite interesting, because none of them have clear optical identifications. Hereafter, we call these objects as Meter-wave Luminous Objects (MLOs). They are considered to have extremely steep radio spectra (with spectral index $\alpha \gtrsim 2$, where $I_\nu \sim \nu^{-\alpha}$), so that they are not detectable at 1.4 GHz. They are supposed to be remnants of merging galaxies (Condon 2005), radio halos and relics (Cohen et al. 2006), or ultra-steep-spectrum radio sources (USSRs; Gopal-Krishna et al. 2005). A sample of MLOs may also involve Galactic objects (such as pulsars, M-dwarfs, and possibly radio-loud extra-solar planets). Because the nature of MLOs is not well known, it is important to establish the association of MLOs to the known objects.

Radio relics are diffuse radio sources which are located at the peripheral regions of clusters of galaxies [often called as "gisht"; see a review by Kempner et al. (2004) and Giovannini & Feretti (2004)]. To date, approximately 30 radio relics have been mapped at 1.4 GHz/325 MHz with VLA or at 610 MHz with GMRT. They are known to have very steep spectral indices ($\alpha \gtrsim 1.5$), and are usually located at peripheral regions of clusters of galaxies without any clear optical counterparts. They are extended by 0.1–1 Mpc in scale and one or two (double) relics are often associated with a cluster. Their radio emissions are polarized by 10–30 percents ($B = 0.1 \sim 1 \mu$ Gauss was suggested). They are quite different from radio halos of clus-

ters of galaxies, which are normally centered to the dense part of a cluster and are often accompanied by X-ray halos. They are also very different from ultra-steep spectrum radio sources (USSRS), which are relatively compact and are identified to optical galaxies (Gopal-Krishna et al. 2005). The origin of radio relics is believed to be dying synchrotron emission produced by shocks between merging clusters of galaxies (e.g., Hoeft & Bröggen 2007). Radio relics share the same properties as MLOs noted above, although the observed frequencies concerned are slightly different.

We identified about 400 MLOs in the VLSS surveyed region by comparing the VLSS and NVSS catalogs, and found that the sample exhibits several strong concentrations in a-few-degree scales in the sky. In this paper, we argue that the cluster appearance of the MLOs toward Monoceros is consistent with what has been seen in higher frequency observations of radio relics in distant clusters of galaxies. The clusters of galaxies with radio relics, which were studied at higher frequencies in the past, are relatively distant ($z \gtrsim 0.05$), because of the smaller field of view of the telescopes at the concerned frequencies (about a degree). In contrast, the scale of newly found clustering of sources at 74 MHz in this paper goes up to about 10 degrees in diameter. The relics spreading in such large angular scales have never been studied at higher frequencies. Therefore, we present the investigation of the Monoceros clustering of MLOs in this paper, and compare the properties with those of known relics in clusters. We conclude that the clustering of 74 MHz sources toward Monoceros is interpreted as aged radio relics associated with the relatively close cluster of galaxies.

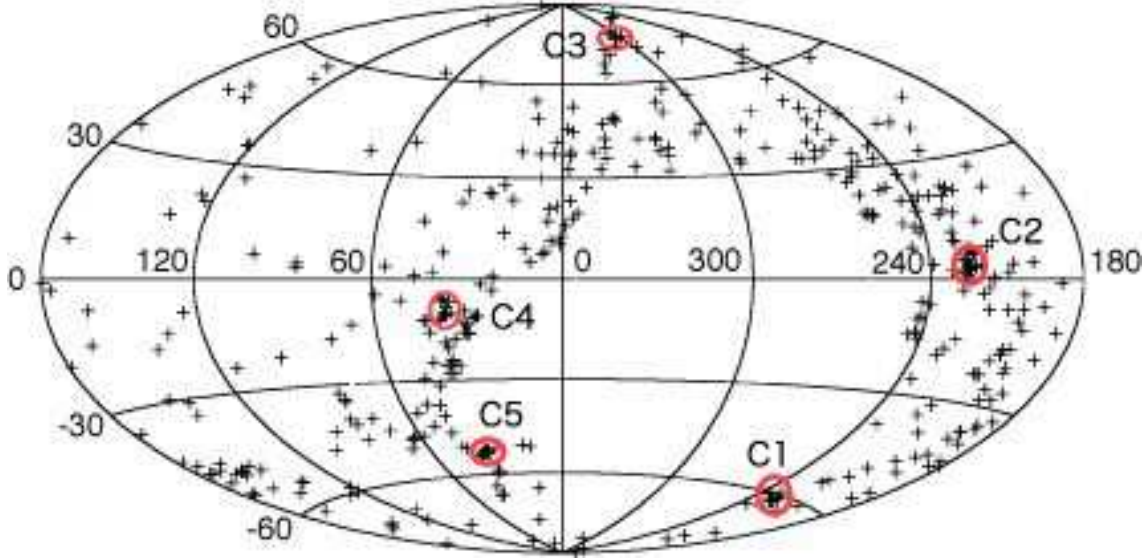


Fig. 1. Distribution of the meter-wave luminous objects in the Galactic coordinates in the Hammer-Aitoff projection. The cross indicates the position of MLO. The possible concentrations of MLOs are marked by ellipses C1 – C5.

2. Sampling of meter-wave luminous objects from the VLSS catalog

The VLSS catalog contains about 68000 radio sources, which were detected with VLA at 74 MHz with $358\ 14^\circ \times 14^\circ$ continuum images (Stokes I) (Cohen et al. 2007). It covers the entire sky north of -30° declination. The flux density limit is approximately 0.7 Jy. The positional accuracy of the source is about $20''$ (95 % significance; see figure 3 of Cohen et al. 2007). This is the most complete, most wide-coverage catalog at low frequencies available at present. From this catalog, we extracted the radio sources without higher frequency detections (within a $80''$ separation). For such a purpose, we used the NVSS catalog, which were also made with VLA at 1.4 GHz (Condon et al. 1998). It covers almost the same area of the sky observed by VLSS, and spatial positions of the VLSS sources were aligned using the NVSS catalog positions identifying the same objects. The NVSS catalog contains about 2 million discrete sources and the detection limit is about 2.5 mJy. The NVSS images have $45''$ angular resolution (FWHM), which is compared with the VLSS image resolution ($80''$).

Because the sensitivity of the NVSS survey exceeds that of the VLSS by a factor of more than 100, the VLSS objects without NVSS detections are in general bright (a few Jy) at 74 MHz (4 m), but extremely faint at 1.4 GHz (21 cm), suggesting that they have very high spectral indices ($\alpha \geq 2$). Therefore, we call these radio sources as Meter-wave Luminous Objects (MLOs). We first selected 499 such objects from the VLSS and NVSS catalogs. However, we noticed that some of the strong sources without the NVSS counterparts in this primary list of MLOs are likely to be false (or time variable sources). It has been known that radio observations at very low frequencies are considerably influenced by ionospheric transmission, and by the large side-lobe interference effect of the strongest

sources, such as Cyg A, Virgo A and the Galactic Center. The positional (phase) errors due to variations of ionospheric transmission were corrected in the VLSS catalog, using the NVSS source positions for the phase calibration (Cohen et al. 2007). However, the sidelobe interference effect does not seem to be completely removed. Cohen et al. (2007) claimed to remove all false detections due to the Gaussian noise by introducing the 5σ peak brightness criterion, and further false detections due to sidelobe interferences by applying the 6σ peak brightness criterion in the vicinity of sources with high peak brightness within a radius of

$$\theta_r = (1^\circ) \sqrt{(I_p / 60 \text{ Jy beam}^{-1})}, \quad (1)$$

where I_p is the peak flux density per beam of a strong source (above 12 Jy beam^{-1}). Even if this procedure removed a considerable number of false detections, we think that it was not enough. The VLSS catalog still contains 5 objects above 50 Jy and 20 objects above 5 Jy, which have no counterparts in the NVSS catalog. These bright objects are likely false detections, because they are located very near to the bright interfering sources (we can visually inspect their contour maps available in the VLSS Postage Stamp Server¹); otherwise, they have much lower flux densities or time-variable flux densities.

In order to improve the reliability of the MLO sample, we also applied the equation (1) for the selection criteria and removed all the objects within θ_r of the strong sources above 12 Jy beam^{-1} . Thus, we selected 416 MLOs from the VLSS and NVSS catalogs, and used this MLO sample for the later analysis.

Figure 1 shows the distribution of MLOs in the Galactic coordinates. The large vacant area around $l = 330^\circ$ and $b = 0^\circ$ is the sky area not accessible from the VLA site

¹ available at <http://www.cv.nrao.edu/4mass/VLSSpostage.shtml>

Table 1. MLO Cluster Candidates.

No.	assignment	l ($^{\circ}$)	b ($^{\circ}$)	r ($^{\circ}$)	number ($n[S/N > 6]$)	density (deg^{-2})	comment
C1	0300–3130	229.1	–61.4	3	12 (7)	0.42	void near Fornax supercluster
C2	0728–0900	225.1	3.9	4	20 (7)	0.40	Monoceros, near the north pole of SGP
C3	1254+1315	305.3	76.1	1.5	5 (2)	0.71	near Virgo A
C4	1933–0022	37.4	–9.4	3.5	9 (4)	0.23	sparse, near the south pole of SGP
C5	2212–2100	33.7	–53.2	3	10 (0)	0.35	false feature ?

($\delta < -30^{\circ}$). The MLOs are clustered at several locations which are indicated by circles C1 – C5. Table 1 summarizes the center coordinates, radius, the number of MLOs, and average surface number density of these concentrations; between the parentheses in column 6, the number of MLO with a high signal-to-noise ratio above 6 is shown. For the choice of concentration features, we use rather a rough criterion in this paper, i.e., more than 5 MLOs are found within a few degree radius. Because the average surface number density of the MLOs between $-30^{\circ} < \delta < 0^{\circ}$ is approximately 0.027 per square degree, the density of MLO for selected clusters is more than 10 times the average except the cluster C4 (which is only about 8 times the average). However, we noticed that the contour map toward concentration C5 (available in the VLSS postage stamp server; e.g., see the $3^{\circ} \times 3^{\circ}$ $25''$ resolution contour map) exhibits a narrow ripple in source distribution; 4 of the 7 members near the center of concentration C5 are aligned on a straight line coming from 2214.4–1701 (about 3° away), suggesting that they are on an interference feature. Therefore, a presence of the concentration C5 is questionable. These rippling structures appear due to insufficient UV coverage and incomplete deconvolution (CLEAN) procedure in the VLA observations.

In the present MLO sample, 269 sources out of 416 MLOs are in the southern hemisphere (occupying only 1/3 of the observed sky area). In the original VLSS catalog, we found that the ~ 62000 sources with high signal-to-noise ratio ($> 6\sigma$ in the integrated intensity S_i) show a distribution with good north-south symmetry, but the ~ 860 VLSS sources with low signal-to-noise ratio ($< 5.5\sigma$) show a marked asymmetry biased toward the southern hemisphere (a factor of 2–3 in density). In fact, the south-bias tends to appear more to the higher noise-level group (with high flux densities $S_i > 1$ Jy) than does to the lower noise-level group (with lower flux densities $S_i < 1$ Jy) in the same low S/N subsample. Therefore, we suspect that the apparent enhancement of the MLO density in the southern hemisphere is a problem of the VLSS detection thresholds in the high noise-level areas, which appear preferentially in the southern hemisphere (partially due to insufficient UV coverage and more deconvolution errors, and partially due to no overlapped mapping areas near the south boundary of the sky coverage; see section 5.2 of Cohen et al. 2007). A substantial fraction of the low S/N southern MLOs could be false sources. The credibility of individual sources and clusters must be assessed carefully. If we remove the objects with low signal-to-noise ratios below

6, the south bias of the MLO distribution is slightly mitigated, though the total number of the remaining MLOs is decreased to 132 (in which 76 are in the southern hemisphere; the subsample still cannot be free from this bias). If we apply the 6σ criterion for the MLO selection, there still remain 7 objects in the concentration C2,² though statistical significance of the other clusters except C1 and C2 is lost. Therefore, in this paper, we only discuss on the largest and strongest concentration C2. The noise level is moderately low toward C2 (close to the average of the ~ 64000 VLSS sources below 5 Jy), but not toward the other clusters. Our visual inspections of the contour maps were well made and all of the sources in C2 listed in table 2 seem to be real.

We also tried to identify the optical/infrared counterparts for the MLOs using Digitized Sky Survey (DSS), Sloan Digital Sky Survey (SDSS), and Two-micron All Sky Survey (2MASS). However, we found that none of MLOs have evident optical/infrared galaxy counterparts within $20''$. A few sources are identified with pulsars within a $5''$ positional separation from the VLSS positions. A few sources have relatively bright stellar candidates. However, the number of sources with a stellar candidate within $10''$ (64% confidence level) increases with the limiting magnitude of candidate stars, and the number also decreases with $|b|$, suggesting that most of them are chance coincidence of stars along the line of sight. From these facts, we deduce that only a few Galactic stars emitting 74 MHz continuum are involved in the present MLO sample. From these studies, we believe that most of MLOs in the present sample are extragalactic objects, such as radio relics and halos.

3. Monoceros concentration of MLOs.

As mentioned in the previous section, some of the concentrations listed in table 1 might be somewhat uncertain. However, C2, the largest concentration (20 sources) toward Monoceros spreading in about 9 degree (see fig-

² If all 44 MLOs found within a $30^{\circ} \times 30^{\circ}$ area toward concentration C2 are randomly distributed, the probability of more than 16 objects falling in the circle of $r = 4^{\circ}$ is less than 10^{-9} , while it is about 1 percent for more than 7 objects being found in the same circle. If we take the 6σ criterion for source selection, the probability of 7 high S/N sources falling into the circle of 4° radius is 2.2×10^{-6} when total 13 high S/N sources within a $30^{\circ} \times 30^{\circ}$ area in this direction are randomly distributed. Therefore, we conclude in both cases that the concentration of C2 is not a result of statistical fluctuations.

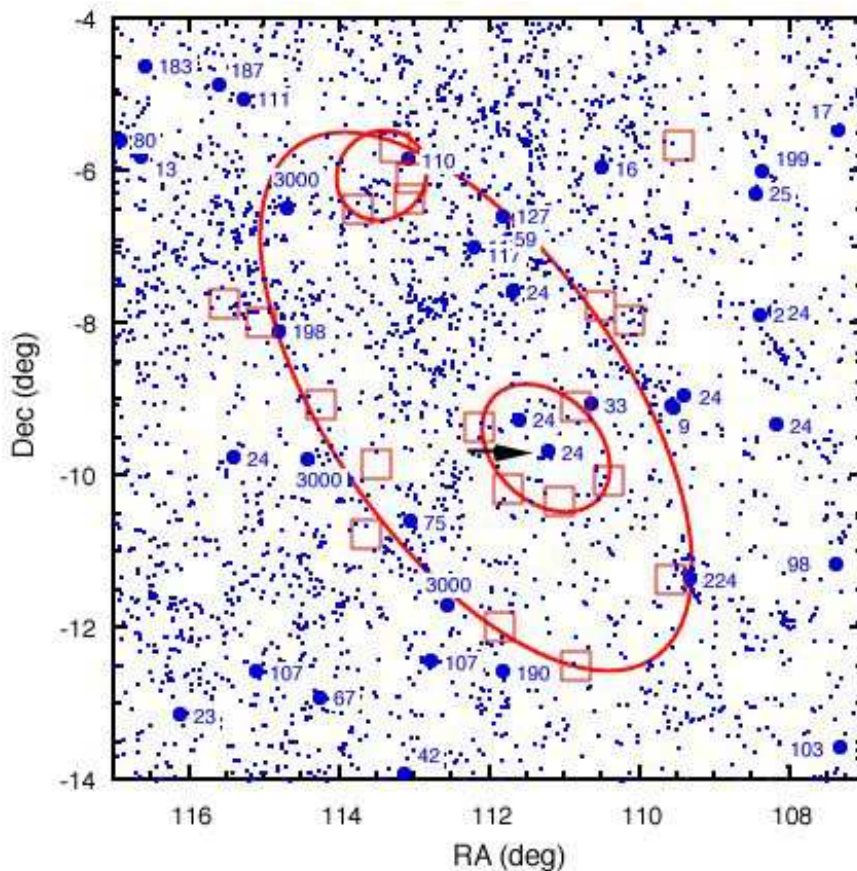


Fig. 2. Distribution of the meter-wave luminous objects (red squares) toward Monoceros in the equatorial coordinates (J2000). Blue dots are the NED galaxies identified in the optical/infrared wavelengths, and blue filled circles the galaxies with known redshifts (the value of cz is written in blue in unit of 100 km s^{-1} , but "3000" indicates $cz > 300000 \text{ km s}^{-1}$). The red ellipses are possible shell structures (see in the text). The position of NGC 2377 ($=3\text{C}178$), is indicated by the arrow.

ure 2), is real. Table 2 lists their positions, flux densities in the VLSS catalog, and the lower limit of the spectral index assuming the sensitivity limit of 2.5 mJy in the NVSS survey. There is no nearby strong interference radio source (except 3C178 [=NGC 2377] with 18.7 Jy at 74 MHz). Because it is roughly toward the Galactic anti-center direction ($l = 225^\circ$), diffuse synchrotron emission in the Galactic plane is expected to marginally contaminate the VLSS sample. However, the close location of this concentration to the Galactic plane ($b = 4^\circ$) makes optical identifications to galaxies somewhat difficult. In 1990s, Saito et al. (1990) found that a large number of galaxies were identifiable in the Palomar Sky Survey plates toward this direction. Yamada & Saito (1993) measured the redshift of several IRAS galaxies in this direction and found that there is a concentration of galaxies at $cz \sim 13000 \text{ km s}^{-1}$ (they call this concentration as the Monoceros supercluster). Although the direction of this supercluster is coincident with the position of MLO concentration C2, we think that they are not physically associated by several reasons described below.

Histogram of redshifts of the galaxies toward Monoceros

(figure 3) indicates that the galaxies in this direction are separated into three major groups: the near one with $cz = 2200 - 2400 \text{ km s}^{-1}$, the middle group with $cz = 10000 - 12000 \text{ km s}^{-1}$, and the far group with $cz = 18000 - 20000 \text{ km s}^{-1}$. These three are different clusters of galaxies; the nearest one is a cluster of galaxies in the Local Supercluster, the second is the Monoceros supercluster (Yamada & Saito 1993), and the third is, we call, the Monoceros NE cluster, because the center of this cluster with $\sim 18000 \text{ km s}^{-1}$ [around $(\alpha, \delta) = (115^\circ, -5^\circ)$] is shifted north-east to the center of MLO concentration C2 (see figure 2). It is possible that the MLO concentration toward Monoceros originates from one of these clusters, or from several clusters by a chance coincidence along the line of sight.

A clue to solve the origin of this MLO concentration is an inner ring of 5 MLOs shown by the small ellipse in figure 2. At the center of this ellipse, the HII galaxy NGC 2377 is located (indicated by the arrow). This is a well studied spiral galaxy (Sbc) with $cz = 2449 \text{ km s}^{-1}$, and one of strong low-frequency radio sources (3C 178; e.g., Haschick et al. 1980). There are also several large

Table 2. Clustered sources toward Monoceros.

VLSS name	l ($^{\circ}$)	b ($^{\circ}$)	F.D. (Jy)	α_L^*
0718.0–0539	221.004	3.300	1.28	2.12
0718.3–1120	226.085	0.720	0.88	1.99
0720.5–0757	223.343	2.792	1.04	2.05
0721.6–1002	225.318	2.052	1.12	2.08
0722.1–0746	223.354	3.218	1.25	2.11
0723.4–1229	227.671	1.275	0.88	1.99
0723.4–0904	224.667	2.889	2.36	2.33
0724.2–1019	225.862	2.485	1.15	2.09
0727.0–1009	226.048	3.163	1.60	2.20
0727.5–1158	227.692	2.398	1.25	2.11
0728.6–0921	225.516	3.886	1.14	2.08
0732.1–0604	223.030	6.219	0.93	2.01
0732.2–0620	223.291	6.110	0.90	2.00
0733.1–0541	222.798	6.604	1.07	2.06
0734.0–0949	226.577	4.845	0.93	2.01
0734.6–1046	227.472	4.516	1.00	2.04
0735.1–0628	223.734	6.667	1.08	2.06
0737.0–0902	226.236	5.855	1.07	2.06
0740.2–0757	225.658	7.065	1.29	2.12
0742.2–0744	225.702	7.614	0.94	2.02

* Lower limit of the spectral index calculated from the sensitivity limit in NVSS of 2.5 mJy.

angular-size galaxies near NGC 2377, though their redshifts are not known (except LEDA 77124 and 2MASX J07263371–0913541; the latter was detected by HI 21cm). The average angular separation of the 5 MLOs to the ellipse center is approximately 1.5 degree.

We compare this value with the angular separation of a proto-typical radio relic in A 521 (Giacintucci et al. 2006) and those in RXC J1314.4–2515 (Venturi et al. 2007). They are detected with GMRT at 610 MHz by ~ 23 mJy beam $^{-1}$ with $HPBW = 15'' \times 13''$ for A 521 ($z = 0.247$), and by ~ 16 mJy beam $^{-1}$ with $HPBW = 15'' \times 13''$ for RXC J1314.4–2515 ($z = 0.2474$). Though the relic sources for these two are not listed in the VLSS catalog, the VLSS contour maps at 74 MHz apparently show enhanced emission of about 0.5 Jy beam $^{-1}$ at the positions of these relics. The angular separation of these relics to the cluster center (approximately 5') can be scaled with redshift as,

$$\theta_s \approx 5'(0.247/z) = 1^{\circ} [6200 \text{ km s}^{-1}/(cz)], \quad (2)$$

where $z \ll 1$. The separation of 1.5° of the Monoceros ring near NGC 2377 is comparable and consistent with the scaled separation, 2.6° , of these prototypical radio relics at $cz \sim 2400 \text{ km s}^{-1}$, if we allow the-line-of-sight orientation effect of the separation by about 50%.

Similarly, we can scale the flux density of the typical relics at the distance of the 2400 km s^{-1} cluster. If we assume that they are point-like at $z = 0.247$, the total flux density, if it is placed at the distance of $cz = 2400 \text{ km s}^{-1}$, should be about 250 Jy at 74 MHz, which is much larger than the sum (~ 6 Jy) of peak flux densities of the ringed 5 MLOs towards NGC2377; even if we include all 20 MLOs

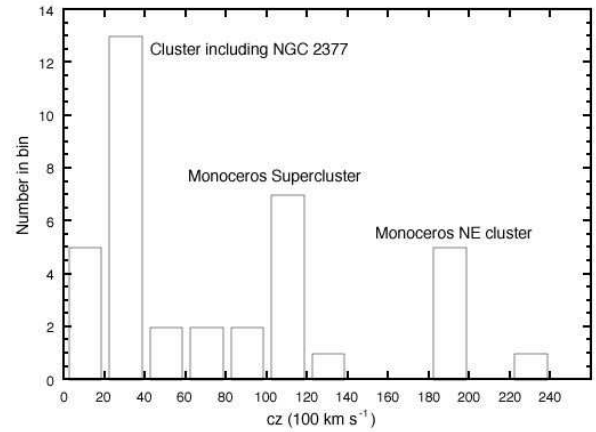


Fig. 3. Histogram of the radial velocity (cz) for the galaxies with known redshift toward Monoceros concentration. All the galaxies with known redshifts are counted in a $10^{\circ} \times 10^{\circ}$ area centered at $(l, b) = (225^{\circ}, 4^{\circ})$. The redshift data were taken from the NASA Extragalactic Database (NED).

of the concentration C2, it only goes up to 23 Jy, though the exact evaluation of the total flux density is difficult because they are not really point-like. However, because the low-frequency emission of relics is deduced to be very extended (in a few degree) and diffuse at such a small distance, it is possible to interpret that the giant relic was fully resolved and most of the 74 MHz flux was missing in the VLSS interferometric observations. Only a few bright patchy portions of filaments are possibly detectable in the VLSS observations³. In fact, very filamentary, giant ringlike double relics without radio halo have been found in Abell 3667 ($z = 0.055$) and 3376 ($z = 0.046$) with ATCA or GMRT, respectively, at 1.4 GHz (Rottgering et al. 1997; Bagchi et al. 2006). Unfortunately, no 74 MHz images are available for these objects because of their low declinations ($\delta < -39^{\circ}$).

Therefore, the MLOs along the inner ellipse in figure 2 are likely to be radio relics associated with the galaxy cluster group (at $cz = 2400 \text{ km s}^{-1}$) centered on NGC 2377. In contrast, the origin of the outer ring of MLOs (the outer large ellipse in figure 2) is much harder to deduce. It might be an outer shell/ring structure of the galaxy cluster centered on NGC 2377. The separations of MLOs from the center of the ellipse are between 1.7° and 4.1° (semi-minor and semi-major diameters of the ellipse). Considering that above scaling formula gives a separation of 2.6° at the NGC 2377 distance, and allowing for the-line-of-sight orientation effect of the separation, we can say that they are also a part of radio relics associated with the 2400 km s^{-1} galaxy cluster. Instead, if they are associated with the Monoceros supercluster, which has $cz \sim 13000 \text{ km s}^{-1}$, their separation is about 3.5–8.5 times larger than the typical separation between

³ In table 2, the brightest source, 0723.4-0904 (2.36 Jy), was resolved in VLSS, but not for the other sources. This is probably because of a low brightness of the extended emission.

relics and the cluster center. Therefore, in the condition that all of these clustered MLOs belong to a single physical entity, we think that these MLOs are not radio relics in Monoceros supercluster at $cz = 13000 \text{ km s}^{-1}$ or beyond.

However, note that above argument does not exclude the possibility that a few of these MLOs are radio relics associated with more distant clusters by chance. A positional coincidence rate of distant MLOs on the nearby MLO concentration can be calculable (see footnote 2). We computed that the number of background sources does not exceed 7 at most in the 20 MLOs in this concentration.

There is a small concentration of 4 MLOs around $(\alpha, \delta) = (113.5^\circ, -6^\circ)$ in figure 2 (the small ellipse in the upper part of figure 2). However, the redshifts have not been measured for the surrounding galaxies except 2MASX J07322365–0548442 at 11063 km s^{-1} (Yamada & Saito 1993). The approximate separation of MLOs from the center of the second ellipse is about 0.5° , which is not inconsistent with the scaled separation of relics to the cluster center if it is associated to the Monoceros supercluster at $cz \sim 13000 \text{ km s}^{-1}$.

One of MLOs, 0718.3–1120 (the lower right red square near blue circles assigned as 224 in figure 2), is located within $15'$ from the X-ray cluster CIZA J0717.4–1119 (Ebeling et al. 2002). The redshift of this X-ray cluster is $z = 0.0750$ ($cz = 22500 \text{ km s}^{-1}$), considerably distant from the other two nearby clusters in this direction. The separation of $15'$ from the X-ray cluster center is coincident with the scaled separations of the relics to the cluster center in A 521 and RXC J1314.4–2515. Therefore, we cannot exclude the possibility that VLSS 0718.3–1120 is a radio relic associated with the X-ray cluster CIZA J0717.4–1119.

The Monoceros concentration of MLOs suggests a presence of a relatively nearby rich galaxy cluster with a 10° scale at $cz \sim 2400 \text{ km s}^{-1}$ in this direction, though it does not reveal clearly in figure 2. Because it is close to the Galactic plane, the past searches for galaxies and measurements of redshifts are quite limited in this region. Visvanathan & Yamada (1996) investigated the distribution of galaxies behind the Milkyway in the area, $210^\circ < l < 360^\circ$ and $|b| < 15^\circ$. Their figure 4 shows that the dense concentration of galaxies with velocities between 1700 and 3200 km s^{-1} is extended at $l = 235 - 245^\circ$ in the $b < 0$ side, but not much between $l = 220 - 230^\circ$ in the $b > 0$ side, where the Monoceros MLO concentration (C2) was found. It is possible that the hypothetical galaxy cluster centered on NGC 2377 at $b = 4^\circ$ is a part of above mentioned large cluster extended in the $b < 0$ side, or it is a cluster colliding and merging with this large cluster. In summary, the MLO concentration can be used as a tracer of relatively nearby galaxy clusters.

4. Conclusion

We investigated the distribution of the meter-wave luminous objects in the sky, and found concentrations of these objects in several directions. In particular, the largest concentration of 20 objects toward Monoceros is

used as a clue to clarify the origin of the clustering. We conclude that these are a part of filamentary structure of giant radio relics associated with the galaxy cluster at $cz = 2400 \text{ km s}^{-1}$, although a few sources might be radio relics contaminated from the distant background clusters. This fact implies that MLOs detectable at the current sensitivity of VLA at 74 MHz are useful to map the structure of the Local Supercluster and its vicinity.

The authors thank Drs. T. Yamada and H. Nagai for helpful comments. This research made use of the SIMBAD and VISIER databases operated at CDS, Strasbourg, France, as well as data products from NASA Extragalactic Database (NED) at JPL funded by the National Aeronautics and Space Administration and the National Science Foundation.

References

- Bagchi, J. Durret, F., Neto, G., B. L., & Paul, S., 2006, *Science*, 314, 791
- Cohen, A. S., Lane, W. M., Lazio, T. J. W., Kassim, N. E., Perley, R. A., Cotton, & W. D., Condon, J. 2005, "X-ray and Radio Connection" proc. E8.08 1
- Cohen, A. S., Lane, W. M., Cotton, W. D., Kassim, N. E., Lazio, T. J. W., Perley, R. A., Condon, J. J., & Erickson, W. C. 2007, *AJ*, 134,1245
- Condon, J. J. 2005, *ASPC*, 345, 237
- Condon J.J., Cotton W.D., Greisen E.W., Yin Q.F., Perley R.A., Taylor G.B., & Broderick J.J. 1998, *AJ*115, 1693
- Ebeling, H., Mullis, C. R., & Tully, R. B. 2002, *ApJ*, 580, 774
- Giacintucci, S., Venturi, T., Bardelli, S., Brunetti, G., Cassano, R., & Dallacasa, D. 2006, *New Astron.*, 11, 437
- Giovannini, G. & Feretti, L. 2004, *JKAS*, 37, 323
- Gopal-Krishna, Ledoux, C., Melnick, J., Giraud, E., Kulkarni, V., & Altieri, B. 2005, *A&A*, 436, 457
- Haschick, A. D., Crane, P. C., Greenfield, P. E., Burke, B. F., & Baan, W. A. 1980, *ApJ*, 239, 774
- Hoefl, M. & Bröggen, M. 2007, *MNRAS*, 375, 77
- Kempner, J. C., Blanton, E. L., Clarke, T. E., Enßlin, T. A. Johnston-Hollitt, M., & Rudnick, L. 2004, in the *Proceeding of The Riddle of Cooling Flows in Galaxies and Clusters of Galaxies*, page 335, edited by T.H. Reiprich, J. C., Kempner, and N. Soker, (Univ. Virginia, Charlottesville)
- Rottgering, H. J. A., Wieringa, M. H., Hunstead, R. W., & Ekers, R. D. 1997, *MNRAS*, 290, 577
- Saito, M., Ohtani, H., Asonuma, A., Kashikawa, N., Maki, T., Nishida, S., & Watanabe, T. 1990, *PASJ*, 42, 603
- Venturi, T., Giacintucci, S., Brunetti, G., Cassano, R., Bardelli, S., Dallacasa, D., & Setti, G. 2007, *A&A*, 463, 937
- Visvanathan, N. & Yamada, T. 1996, *ApJS*, 107, 521
- Yamada, T. & Saito, M. 1993, *PASJ*, 45, 25